

Axial flux machine performance enhancement using recurrent neural network controller

Kalpana Anumala, Ramesh Babu Veligatla

Department of Electrical and Electronics Engineering, VNR Vignana Jyothi Institute of Engineering and Technology (VNRVJIET),
affiliated to Jawaharlal Nehru Technological University (JNTU), Hyderabad, India

Article Info

Article history:

Received May 21, 2024

Revised Jan 17, 2025

Accepted Mar 1, 2025

Keywords:

Dual rotor axial flux induction motor

Learning rate

Long short-term memory controller

Multi-level inverter

Recurrent neural network

ABSTRACT

Traditional control methods often face limitations in optimizing the performance of these motors, especially in complex industrial and automotive applications where precision, stability, and energy efficiency are paramount. By exploring advanced control strategies such as multi-level inverters and neural network controllers, this study aims to overcome these limitations and unlock the full potential of dual rotor axial flux induction motors. The integration of multi-level inverters enables finer control of motor operation and enhances power quality, while neural network controllers offer adaptive and intelligent control capabilities, enabling the system to learn and optimize performance in real-time. The study investigates novel approaches to enhance the performance and efficiency of electric motor control systems. The study aims to address the challenges associated with traditional control methods and optimize the operation of dual rotor axial flux induction motors. The research evaluates various performance metrics associated with the speed control system, including error histograms, training performance, regression accuracy, rotor speed dynamics, rotor torque characteristics, time series analysis, and training state assessment. The study achieves significant milestones in optimizing system performance, as evidenced by key findings such as a low mean squared error (MSE) of 0.00011396 achieved during training, strong correlation in regression analysis with an R-value of 0.99718, and effective training dynamics indicated by a gradient value of 0.0091742 and a learning rate (μ) of 0.0001. These results underscore the effectiveness and reliability of the proposed control strategies in improving motor performance, efficiency, and reliability while reducing energy consumption and operational costs. The proposed method is implemented using MATLAB.

This is an open access article under the [CC BY-SA](#) license.



Corresponding Author:

Kalpana Anumala

Department of Electrical and Electronics Engineering

VNR Vignana Jyothi Institute of Engineering and Technology (VNRVJIET)

affiliated to Jawaharlal Nehru Technological University (JNTU)

Hyderabad, India

Email: anumala.kalpana@gmail.com

1. INTRODUCTION

In light of the intricate dynamics of induction motors, a controller that can deliver reliable control must be in place. Additionally, induction motor controllers provide the electro-mechanical system with monitoring and safety [1]. It is necessary to understand the dynamic physical representation of induction motors to use these services. The foundational ideas of physics are the source of accurate dynamics [2]. These dynamical models rely on many physical properties of induction motors, such as prevailing currents, voltages, fluxes, inductances, and voltages, which may be monitored in either direct or indirect ways with the

use of estimators or sensors [3]. Because of noise and operating circumstances, monitoring some of these values accurately is difficult. Physical model-based controllers are very dependable and are used extensively in industry [4]. While there are simulations of the induction motor with minimal complexity, they are nonlinear and have several unknown parameters. The industrial internet of things, a lot of data from various electro-mechanical equipment, may now be collected [5]. Online decision methods for electric system monitoring applications have been made possible by the induction motor systems' real-time or almost real-time data collection. Improved prediction models have also resulted from recent developments in deep neural networks used for longitudinal research [6]. The utilization of techniques such as convolutional neural networks, artificial neural networks, and LSTM architectures has facilitated the end-to-end learning of temporal dynamics from time-series data [7]. In electrical motor operations, neural networks have recently been actively employed as controllers, monitors, and failure predictors [8]. The research employed the design of encoder-decoders to extract kinetics from induction motor data [9].

Machine learning measures such as accuracy, R-square, mean square error, and so on are used to assess these techniques. Although these measures have a built-in prejudice towards the dataset, they are well-suited for tasks involving regression and prediction [10]. The research examines the reasons behind the failure of these measurements and suggests a mechanism for appropriately assessing neural network approaches for induction motor issues using electrical engineering metrics in conjunction with quasi-static and dynamic benchmarks. The task of forecasting velocity and electromagnetic torque using current and voltage representations in a (d-q) frame is examined [11]. Proposals have also been made for neural network-based control techniques to develop an improved model that can solve issues with the conventional model-based methodology [12]. Current research uses circular-based neural network models to understand the connection between flux connections and currents [13]. When it comes to electrical motor operations, neural network classifiers are constantly utilized for defect diagnostics [14]. The method learns motor dynamics through simulated data, performs fault recognition in simulated motor activities, and does not employ dynamics modeling; instead, it simply uses supervised labels [15]. It is suggested to use an encoder-decoder network to directly learn electrical motor dynamics from recorded data. The input-output connection is well-modeled by the suggested approach [16]. The extant literature examines the factors for the failure of neural networks. Because neural networks contain many parameters, differing modeling techniques, and fewer assumptions than other models, they present greater opportunities for misuse and troublesome applications [17]. The idea of considering neural networks like black boxes is another significant mistake. To understand neural network outputs in terms of input impacts and connections among variables being input, a robustification approach is presented [11]. Neural networks, because of their huge number of parameters and data-hungry environment, are susceptible to two well-known difficulties in machine learning techniques: under-fitting and over-fitting [18]. Didane *et al.* [19] explained the research and estimation of the aerodynamic efficiency of a special contra-rotating vertical direction wind turbine. This research aims to examine the feasibility of improving a VAWT method's conversion effectiveness by applying the contra-rotating principle. The power, torque, power coefficients, torque coefficients, and other important aerodynamic performance metrics were used to construct the effectiveness assessments of the present model. Taghinezhad *et al.* [20] presented a study that assesses and improves the effectiveness of turbines that generate electricity with two rotors that are mounted inside of a specially designed duct. The input variables for the training samples with the testing samples were acquired, respectively, using the Latin hypercube samples and random sampling having a uniform distribution of imbalance distributions of the fan disc with the hyper-compressor disc [21]. Fu *et al.* [22] use the non-intrusive polygonal form mathematical meta model to examine the non-probabilistic steady-state kinetics of dual-rotor systems with parametric imperfections under two-frequency excitations. The formulas for the equations for the movement of the entire system are obtained using the Lagrangian approach. Kreutz *et al.* [23] explain in detail that the financial viability of wind turbines is decreased by downtime brought on by ice development on the rotor blades. Chen and Hubner [24] provides information on a possible actuator disc theory-based flow the solution for dual-rotor-wing interactions, the method of images, and the theory of momentum about of rotor dragged and wings downloading force of small tilt rotor-like vehicles; the analytical model analyses the impact of rotor height beyond the wing, the rotor disc protection over the wing, and the distance between two rotors; it requires the rotor radius, which helps with initial design studies on tilt rotor-like vehicles; the analytical results agree well with the experimental data regarding magnitude and trend, especially the rotor thrust.

A viable option for improving the effectiveness and performance of electric engine systems is the use of dual-rotor axial flux induction engines, especially in situations where torque variation and constant speed maintenance are crucial. These twin-rotor arrangements are ideal for challenging industrial and transportation applications because they provide special benefits in terms of power density and torque capabilities. Advanced control solutions are necessary to fully realize the promise of dual-rotor axial flux induction motors. This project aims to investigate and create sophisticated control techniques for dual-rotor axial flux induction motors with changing torque needs and constant speed. It will do this by utilizing multi-level inverters and neural network controllers. The integration of MLIs allows for precise modulation of

voltage and current waveforms, enabling efficient control of motor operation. Additionally, the incorporation of artificial neural network controllers offers adaptive and intelligent control capabilities, enhancing the system's robustness and performance under dynamic operating conditions. Furthermore, this study will investigate the potential synergies between MLIs and various neural network-based controllers, including fuzzy logic controllers and long short-term memory (LSTM) controllers, to further optimize the motor's operational efficiency and stability. By combining advanced control techniques with the unique characteristics of dual-rotor axial flux induction motors, this research aims to contribute to the advancement of electric propulsion systems for a wide range of industrial and transportation applications, ultimately fostering sustainability and energy efficiency in the modern era. The proposed controller in this study is the recurrent neural network (RNN) controller, which offers a cutting-edge approach to control systems design and optimization. Unlike conventional controllers such as proportional-integral, fuzzy logic, and artificial neural network (ANN) controllers, RNN controllers leverage the power of recurrent neural networks to handle dynamic and time-varying systems more effectively. The RNN controller benefits from its ability to process sequential data, making it particularly suitable for applications where past states influence current decisions, such as time series prediction and sequential decision-making tasks. Additionally, RNN controllers excel in capturing complex nonlinear relationships within the system, allowing for more accurate and adaptive control in highly dynamic environments. RNNs can learn from historical data and adapt their internal state based on past experiences, enabling improved performance over time as the controller continuously learns and updates its parameters. The proposed RNN controller offers the advantages of enhanced adaptability, improved accuracy, and superior performance compared to traditional control strategies, making it a promising choice for a wide range of control applications in various industries. The rest of the section is organized as follows: i) Section 1 describes the introduction; ii) Section 2 gives the problem statement; iii) Section 3 provides the proposed methodology; iv) Section 4 evaluates the result section; and v) Section 5 gives the conclusion and future work.

2. PROBLEM STATEMENT

The advancement and optimization of control strategies for dual-rotor axial flux induction motors using multi-level inverters and neural network controllers remain an area of active research and development. While dual-rotor systems offer potential advantages in terms of efficiency and power generation, effective control strategies are crucial for maximizing their performance and ensuring reliable operation. However, existing literature primarily focuses on the mechanical and aerodynamic aspects of dual-rotor systems, such as their design, aerodynamic interactions, and power generation capabilities. There is a gap in research concerning advanced control strategies tailored specifically for dual-rotor axial flux induction motors. Despite the potential advantages of dual-rotor axial flux induction motors, there is a lack of research focused on advanced control strategies utilizing multi-level inverters and neural network controllers. This study aims to address this gap by investigating and developing advanced control strategies tailored specifically for dual-rotor axial flux induction motors. The research will focus on enhancing the efficiency, reliability, and performance of dual-rotor systems through the application of advanced control techniques, such as multi-level modulation strategies and neural network-based controllers. Additionally, the study will explore the integration of these control strategies with dual-rotor systems to optimize energy conversion and operational performance under varying operating conditions. The ultimate goal is to contribute to the advancement and optimization of dual-rotor axial flux induction motors for efficient energy conversion and enhanced performance in renewable energy applications [25].

3. PROPOSED RNN CONTROLLERS FOR DUAL ROTOR AXIAL FLUX INDUCTION MOTORS

The proposed methodology focuses on enhancing the control strategies for dual rotor axial flux induction motors (DRAFIMs) by integrating advanced technologies such as multi-level inverters and recurrent neural network (RNN) controllers. The design incorporates electronic circuitry and control system components for managing the differential operation of the dual rotor system, facilitating independent or synchronized control of rotor speeds. Multi-level inverters enable precise control over voltage output, enhancing power quality and efficiency. The use of LSTM controllers optimizes current, torque, and speed regulation in DRAFIMs, ensuring optimal performance under varying load conditions. The proposed methodology offers a comprehensive approach to motor control, promising higher efficiency, reliability, and adaptability across a wide range of industrial and automotive applications.

3.1. Design of dual rotor axial flux induction motors

This system suggests the presence of electronic circuitry or control system components that enable the management and control of the dual-rotor motor. The term "differential system" implies that there might

be a mechanism for controlling or adjusting the speed or torque output of the two rotors differentially, allowing for independent control or synchronized operation. Control circuitry involves microcontrollers, digital signal processors (DSPs), and electronic control units responsible for processing sensor data and generating control signals for the motor. Components like inverters, converters, or motor drives convert electrical energy to mechanical energy and control the speed and torque of the motor. The dual rotor axial flux induction motor has two rotors, each arranged axially on either side of the stator. The axial flux design means that the magnetic flux flows parallel to the motor's shaft, which can offer advantages in terms of efficiency and power density. A dual rotor axial flux induction motor system, when coupled with multi-level inverters, forms a sophisticated subsystem with enhanced performance capabilities. This subsystem combines the unique features of the DRAFIM, known for its compact design and high torque density, with the advantages offered by multi-level inverters in terms of improved voltage quality, reduced harmonic distortion, and increased efficiency. In this configuration, the multi-level inverters facilitate precise control over the voltage supplied to the DRAFIM, enabling optimal operation across various load conditions.

3.2. LSTM controller

In the context of a dual rotor axial flux induction motor (DRAFIM) controlled by a long short-term memory (LSTM) controller, each of the key parameters - current, torque, and speed - plays a critical role in the overall operation and performance of the motor system. The current flowing through the stator windings of the DRAFIM is a fundamental parameter that directly influences motor performance. The LSTM controller monitors and regulates the stator current to maintain desired operating conditions, such as torque production and motor efficiency. The LSTM controller Figure 1 modulates the torque output of the DRAFIM by adjusting the current supplied to the stator windings.

The rotational speed of the motor's shaft is another key parameter controlled by the LSTM controller. By regulating the frequency of the current supplied to the motor windings, the LSTM controller adjusts the motor speed to match the desired operating point. Whether the application requires precise speed control for industrial automation or variable speed operation for vehicle propulsion, the LSTM controller ensures smooth and responsive speed regulation, maintaining stability and efficiency throughout the motor's operating range.

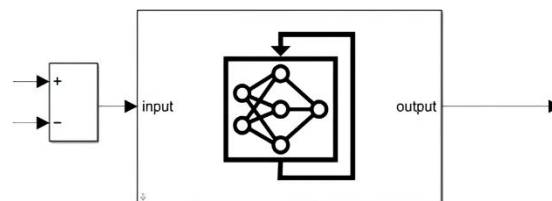


Figure 1. LSTM controller

3.3. Enhanced torque control in dual rotor by employing multilevel inverter fed DRAFIM

MLIs offer finer control over the applied voltage and current waveforms, allowing for better regulation of torque in the DRAFIMs. This capability is essential for achieving precise torque control, which is necessary for various industrial and automotive applications. Enhanced torque control in a dual rotor system is achieved by employing a multilevel inverter-fed transposed resonant AC field induction motor (TRAFIM). This innovative approach enhances the precision and efficiency of torque control by utilizing a multilevel inverter to generate a high-quality voltage supply to the DRAFIM, enabling smoother torque regulation and minimizing torque ripple. The DRAFIM technology, which involves transposing the stator and rotor windings, facilitates better utilization of magnetic flux, resulting in improved torque performance and reduced losses. Additionally, the multilevel inverter allows for finer control of voltage levels, enabling optimized torque output across a wider range of operating conditions. The flux vector end points move along a collinear straight line of the VSI voltage vectors. The new magnitude and phase of the required flux vector at time t_{n+1} depend on the following: i) flux at time t_n , and ii) supplied voltage vectors applied at time t_n . The control strategy defines a required flux reference for each sampling time. The appropriate voltage vector on VSI outputs can be deduced from the estimated values of the two fluxes and the two required fluxes. The total electromagnetic torque (T_e) in a dual-rotor axial flux induction motor can be expressed as the sum of two components caused by the electromagnetic interaction between the stator and each rotor. The motion equation of the wind turbine system derives the torque due to the electromagnetic effect and the mechanical torque. The equations are shown as in (1) and (2).

$$\frac{jd\omega_m}{dt} = T_e - T_m \quad (1)$$

$$T_e = \frac{3P}{2} \text{Re}(j\vec{\lambda}_s \vec{i}_r) = \frac{-3P}{2} \text{Re}(j\vec{\lambda}_s \vec{i}_r) \quad (2)$$

The dual rotor mathematical modeling using dq axis representations and dq frame as a reference conversion. The modeling equations are as in (3)-(8).

$$\vec{V}_s = V_{ds} + jV_{qs} \quad (3)$$

$$\vec{V}_r = V_{dr} + jV_{qr} \quad (4)$$

$$\vec{i}_s = i_{ds} + ji_{qs} \quad (5)$$

$$\vec{i}_r = i_{dr} + ji_{qr} \quad (6)$$

$$\vec{\lambda}_s = \lambda_{ds} + j\lambda_{qs} \quad (7)$$

$$\vec{\lambda}_r = \lambda_{dr} + j\lambda_{qr} \quad (8)$$

In the dq axis frame, the voltage equations for the rotor and stator are as (9)-(12).

$$V_{ds} = R_s i_{ds} + p\lambda_{ds} - \omega\lambda_{qs} \quad (9)$$

$$V_{qs} = R_s i_{qs} + p\lambda_{qs} + \omega\lambda_{dr} \quad (10)$$

$$V_{dr} = R_r i_{dr} + p\lambda_{dr} - (\omega - \omega_r)\lambda_{qr} \quad (11)$$

$$V_{qr} = R_r i_{qr} + p\lambda_{qr} + (\omega - \omega_r)\lambda_{dr} \quad (12)$$

The flux links between both rotor and stator in the reference frame of the dq axis are as (13)-(16).

$$\lambda_{ds} = (L_{ls} + L_m)i_{ds} + L_m i_{dr} = L_s i_{ds} + L_m i_{dr} \quad (13)$$

$$\lambda_{qs} = (L_{ls} + L_m)i_{qs} + L_m i_{qr} = L_s i_{qs} + L_m i_{qr} \quad (14)$$

$$\lambda_{dr} = (L_{lr} + L_m)i_{dr} + L_m i_{ds} = L_r i_{dr} + L_m i_{ds} \quad (15)$$

$$\lambda_{qr} = (L_{lr} + L_m)i_{qr} + L_m i_{qs} = L_r i_{qr} + L_m i_{qs} \quad (16)$$

Equations in the dq-reference frame that illustrate motion resulting from mechanical rotation are as (17)-(19).

$$T_e = \frac{3P}{2}(i_{qs}\lambda_{ds} - i_{ds}\lambda_{qs}) \quad (17)$$

$$T_e = \frac{3P}{2}(i_{qs}\lambda_{qr} - i_{ds}\lambda_{qr}) \quad (18)$$

$$T_e = \frac{3P}{2}(i_{qs}\lambda_{dr} - i_{ds}\lambda_{qr}) \quad (19)$$

3.4. RNN controller for DRAFIM controlling mechanism

The RNN controller in Figure 2 plays a transformative role in motor control systems by harnessing the power of artificial intelligence and machine learning. Unlike traditional control methods, RNN controllers possess the ability to process sequential data and capture temporal dependencies in the system's behavior. As a result, RNN controllers represent a cutting-edge approach to motor control, promising to revolutionize industrial processes and systems by enabling more intelligent and adaptive control strategies.

The reference design for the suggested RNN control framework is selected in accordance with the time-domain parameter values, as seen in Figure 2. In the input, hidden, and output layers of the RNN, there are 2, 20, and 1 neuron respectively. The connecting values are initialized with randomized integers. The position instruction, denoted by $p * r$, is sent into the RNN as inputs, along with $es(1 - z - 1)$; the result of the RNN is the controlling signaling up. Furthermore, simultaneous updates are made to all of the learning pace parameters.

$$\frac{\omega_m^2}{s^2 + 2(\omega_m s + \omega_m^2)} = \frac{6.7244}{s^2 + 5.1863s + 6.7244} \quad (20)$$

Here, S is the Laplace operator, and μ and ω_n are the damping ratio and undamped natural frequency, respectively. In contrast, the model that serves as the reference is set to one when the input is a periodic sinusoidal instruction. The tracking deviation resulting from the plant's condition and the model used for reference is supplied out to train the connecting values of the RNN controller globally, generating a control input for the entire system, as the required commands tracking responses is established in the standard network's output.

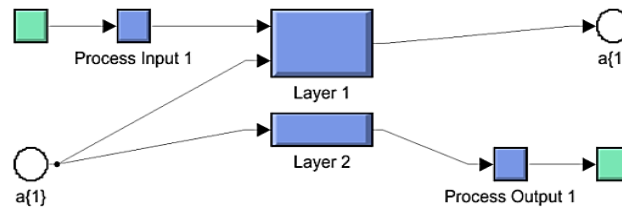


Figure 2. RNN controller

4. RESULTS AND DISCUSSION

The results section encompasses the analysis of various performance metrics associated with a speed control system utilizing an RNN controller. The study evaluates parameters such as error histograms, training performance, regression, rotor speed, rotor torque, time series analysis, and training state. Each analysis provides insights into different aspects of system performance, ranging from error distribution and model training dynamics to electrical current flow, voltage stability, and mechanical behavior. The effectiveness of the proposed study in finding the provided metrics is notable. The error histogram visually represents error distribution, aiding in identifying patterns and discrepancies within the dataset. Regression analysis provides a diagnostic tool for evaluating model accuracy and identifying areas for improvement.

4.1. Output of RNN controller

The comprehensive range of analyses conducted in the study highlights the effectiveness of the proposed methodology in capturing and evaluating various performance metrics essential for assessing the reliability, stability, and efficiency of the speed control system. The insights gleaned from these analyses provide valuable information for system optimization, fault diagnosis, and performance enhancement, demonstrating the significance of the study in advancing the understanding and development of advanced control systems for industrial applications.

4.1.1. Error histogram

The error histogram graph in Figure 3 provides a visual representation of the frequency distribution of errors across different instances or data points. Figure 3(a) shows the distribution of errors (difference between target and output values) in a training model. The histogram indicates that most errors are concentrated around zero, implying that the model's predictions are highly accurate. The blue bars represent training errors, while the orange line represents zero error for reference. Figure 3(b) is an error histogram with 20 bins that shows the distribution of errors (difference between target and output values) for a trained model. The majority of errors are concentrated around zero, as indicated by the tall blue bar, suggesting that the model has high accuracy. Each instance corresponds to a specific error value, plotted along the x-axis, while the y-axis indicates the frequency or number of occurrences for each error. The distribution of errors depicted in the histogram enables a comprehensive understanding of the variability and consistency within the dataset.

4.1.2. Training performance

The training performance graph in Figure 4 presents a visual depiction of the performance of a machine learning model during the training process, with the number of training epochs represented along the x-axis and the mean squared error (MSE) displayed on the y-axis. This graph serves as a critical tool for assessing the model's learning dynamics and convergence behavior over successive epochs. Figure 4(a) shows good training performance, with MSE reducing significantly over time. The best performance is achieved at epoch 1000, training might still be beneficial if extended further. Figure 4(b) shows that in the initial running MSE drops quickly and after 100 epochs, it is constant.

At epoch 1000, the presented value at 0.00011396 reflects the lowest mean squared error achieved by the model throughout the training process up to that specific point. The attainment of a low MSE value at epoch 1000 underscores the effectiveness and progress of the training process. At epoch 1000, the presented value of 0.011606 also reflects the lowest mean squared error.

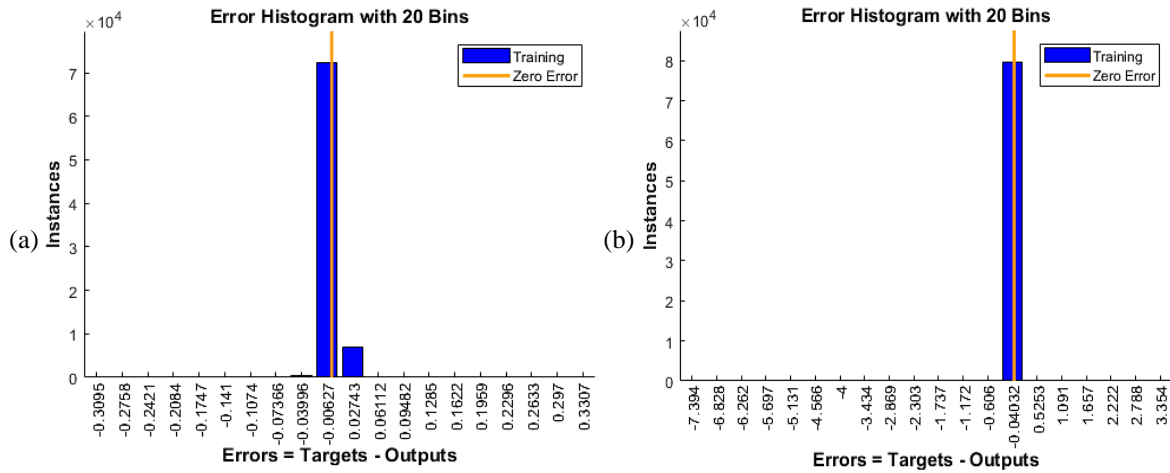


Figure 3. Error histogram: (a) error histogram with 20 Bins (training model) and (b) error histogram with 20 Bins (trained model)

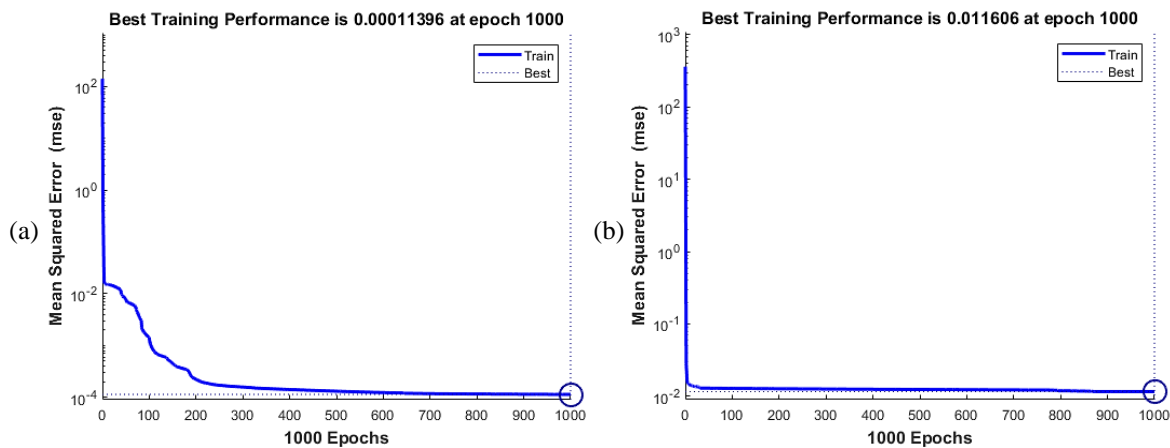


Figure 4. Training performance: (a) training at 0.011606 and (b) training at 0.00011396

4.1.3. Regression

The regression graph in Figure 5, with the target variable plotted on the x-axis and the model's output displayed on the y-axis, provides a visual representation of the relationship between the predicted and actual values in a regression analysis. Figure 5(a) indicates that the model has achieved excellent training performance, with a high correlation coefficient ($R = 0.99718$), meaning the predictions are strongly aligned with the target values. This graph serves as a diagnostic tool for evaluating the performance and accuracy of the regression model. A perfect regression model would exhibit a diagonal line with a slope of 1, indicating that the predicted values perfectly align with the actual target values. Deviations from this ideal line reveal the degree of error in the model's predictions, with discrepancies suggesting areas for improvement such as bias, variance, or model complexity. Figure 5(b) indicates poor training performance, with a relatively low correlation coefficient ($R = 0.65637$).

4.1.4. Rotor speed

The rotor speed graph in Figure 6, with time represented along the x-axis and rotor speed displayed on the y-axis, offers a dynamic visualization of the rotational velocity of a rotor system over a specific

period. This graph provides essential insights into the temporal behavior and performance of the rotor, facilitating the assessment of its stability, responsiveness, and operational characteristics.

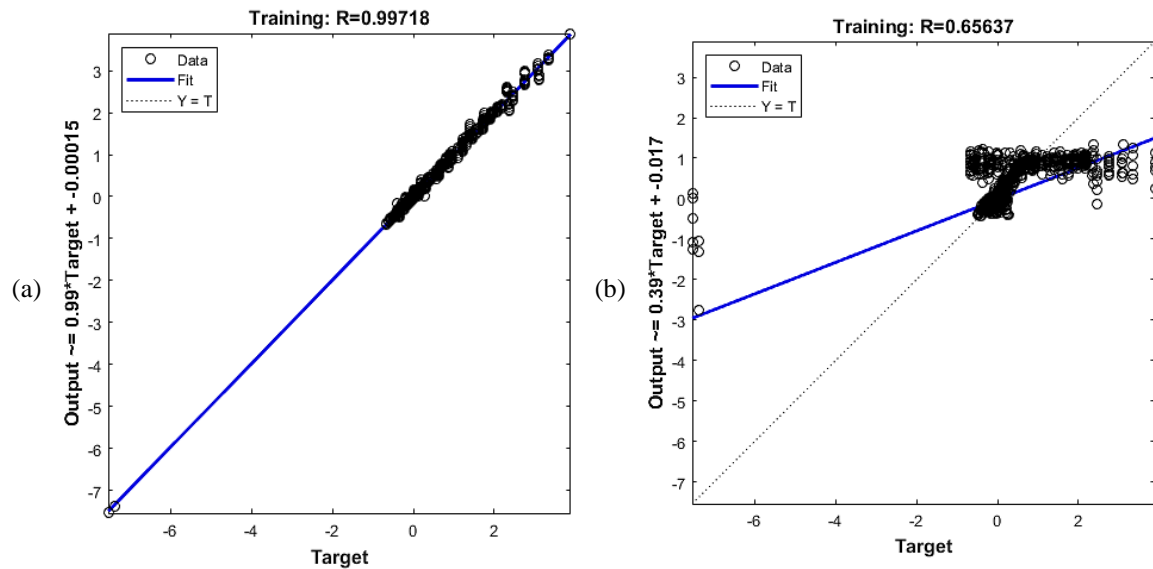


Figure 5. Regression: (a) training at R = 99718 and (b) training at R = 0.65637

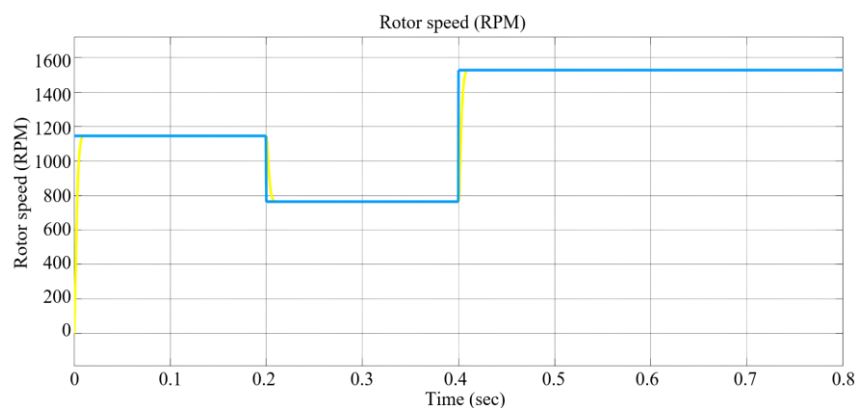


Figure 6. Rotor speed

4.1.5. Rotor torque

The rotor torque graph Figure 7, with time depicted on the x-axis and rotor torque plotted on the y-axis, provides a comprehensive depiction of the torque output of a rotor system over a specified time period. This graph offers crucial insights into the dynamic behavior and performance of the rotor, allowing for the assessment of its mechanical efficiency, load variations, and operational characteristics.

4.1.6. Time series

The time series graph in Figure 8, with time represented on the x-axis and error, output, and target values plotted on the y-axis, provides a dynamic visualization of the temporal behavior and performance of a system or model over a specific duration. Figure 8(a) shows the model's response for output element 1 in a time-series task. The top plot compares training targets and outputs, while the bottom plot shows minimal errors, indicating high model accuracy. Figure 8(b) shows the response of output element 1 in a time-series model, where training targets and outputs closely match. The error remains near zero, indicating the model's high accuracy with minimal deviations. This graph offers valuable insights into the relationship between predicted and actual values, enabling the assessment of the accuracy, precision, and consistency of the model's predictions over time. Figure 8 indicates training targets in actual values.

Table 1 presents a detailed analysis of the performance metrics associated with the speed control system, outlining various parameters such as rise time, peak overshoot, settling time, and maximum speed

reached during peak overshoot for different speed ranges. The table provides insights into the dynamic behavior of the system across different operational scenarios, highlighting the time required to achieve reference speeds, the magnitude of peak overshoot, and the duration for the system to settle at a constant speed.

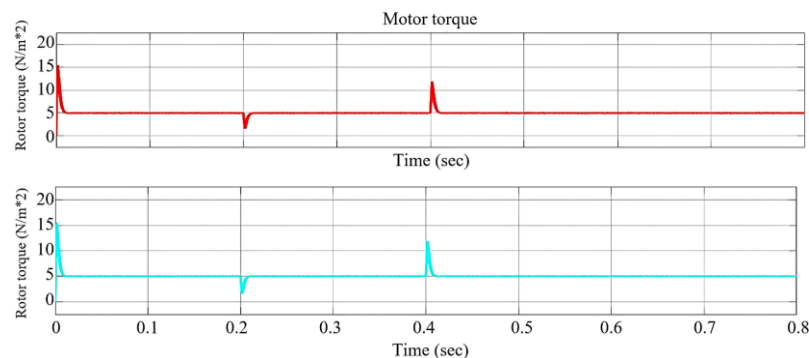


Figure 7. Rotor torque

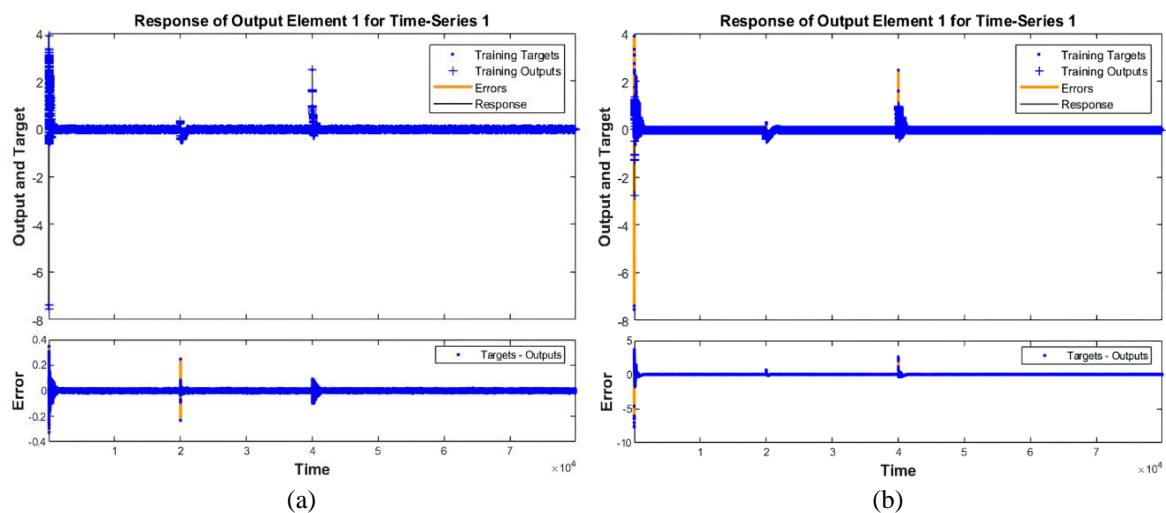


Figure 8. Time series: (a) model performance and (b) response of output element 1

Table 1. Output of RNN controller

| Time | Rise time to reach the reference speed (0-120) | Peak overshoot | Maximum peak overshoot | The settling time to reach a constant value | Maximum speed in peak overshoot | Settlement time |
|-------------------|--|----------------|------------------------|---|---------------------------------|-----------------|
| Starting time (0) | | | | | | |
| To reach 0-120 | 0.009 | 0.01-0.015 | 0.01-0.015 | 0.01-0.015 | 1148 | 0.005 |
| To reach 120-80 | 0.007 | 0.21-0.211 | 0.21-0.211 | 0.21-0.207 | 762.5 | 0.0055 |
| To reach 80-160 | | 0.4-0.408 | 0.4-0.408 | 0.4-0.408 | 1529.5 | 0.055 |

4.2. Discussion

The analysis of the output from the RNN controller provides valuable insights into the performance of the speed control system across various operational scenarios. The rise time, indicating the time taken to reach the reference speed, demonstrates rapid responsiveness, with minimal delays observed across different speed ranges. The peak overshoot metrics reveal slight variations within acceptable ranges, suggesting effective control mechanisms to minimize deviations from the reference speed. Settling times indicate the system's ability to stabilize at the desired speed, with consistent performance demonstrated across different speed transitions.

5. CONCLUSION AND FUTURE WORK

Through the examination of various performance metrics such as rise time, peak overshoot, settling time, and maximum speed reached during peak overshoot across different operational scenarios, we have

demonstrated the effectiveness and reliability of the RNN controller in achieving precise and responsive speed regulation. The results indicate rapid responsiveness, minimal deviations from the reference speed, and consistent performance in stabilizing at desired speeds, showcasing the suitability of the proposed control system for real-world applications where accurate speed control is paramount. There are several avenues for future work to further enhance the efficiency and effectiveness of the speed control system. The exploration of advanced machine learning techniques and optimization algorithms could potentially improve the performance and robustness of the control system, enabling better adaptation to dynamic operating conditions and disturbances.

FUNDING INFORMATION

Authors state no funding involved.

AUTHOR CONTRIBUTIONS STATEMENT

This journal uses the Contributor Roles Taxonomy (CRediT) to recognize individual author contributions, reduce authorship disputes, and facilitate collaboration. All authors contributed equally to the study design, data collection, analysis, and manuscript preparation. All authors have reviewed and approved the final manuscript.

| Name of Author | C | M | So | Va | Fo | I | R | D | O | E | Vi | Su | P | Fu |
|-----------------------|---|---|----|----|----|---|---|---|---|---|----|----|---|----|
| Kalpna Anumala | ✓ | ✓ | ✓ | ✓ | ✓ | ✓ | | ✓ | ✓ | ✓ | | | ✓ | |
| Ramesh Babu Veligatla | ✓ | ✓ | ✓ | | | ✓ | | ✓ | ✓ | ✓ | ✓ | ✓ | | |

C : Conceptualization

M : Methodology

So : Software

Va : Validation

Fo : Formal analysis

I : Investigation

R : Resources

D : Data Curation

O : Writing - Original Draft

E : Writing - Review & Editing

Vi : Visualization

Su : Supervision

P : Project administration

Fu : Funding acquisition

CONFLICT OF INTEREST STATEMENT

The authors declare no conflicts of interest.

DATA AVAILABILITY

The data used in this study were obtained from publicly available sources. Authors are encouraged to provide direct and clear links or references to these datasets to ensure transparency and facilitate reproducibility. In this study, data were sourced from the following publications:

- DOI: 10.1177/00202940231195117
- DOI: 10.5829/ije.2022.35.03C.04
- DOI: 10.46300/91012.2020.14.7
- DOI: 10.1177/0309524X19868423
- DOI: 10.1109/TASC.2020.2977286
- DOI: 10.1016/j.compeleceng.2021.107258
- DOI: 10.1109/TIA.2022.3191300
- DOI: 10.1177/00202940231201375
- DOI: 10.1038/s41598-024-55271-7
- DOI: 10.1109/TMAG.2021.3127359
- DOI: 10.1016/j.cja.2020.01.009
- DOI: 10.1109/ACCESS.2020.3028425
- DOI: 10.3390/electronics10161880
- DOI: 10.1016/j.renene.2017.08.070




REFERENCES

- [1] H. Benbouhenni, N. Bizon, P. Thounthong, I. Colak, and P. Mungporn, "A new integral-synergetic controller for direct reactive and active powers control of a dual-rotor wind system," *Measurement and Control*, vol. 57, no. 2, pp. 208–224, Feb. 2024, doi: 10.1177/00202940231195117.
- [2] H. Benbouhenni, "Amelioration effectiveness of torque and rotor flux control applied to the asynchronous generator for dual-rotor wind turbine using neural third-order sliding mode approaches," *International Journal of Engineering*, vol. 35, no. 3, pp. 517–530, 2022, doi: 10.5829/IJE.2022.35.03C.04.
- [3] J. Si, T. Zhang, Y. Hu, C. Gan, and Y. Li, "An axial-flux dual-rotor slotless permanent magnet motor with novel equidirectional toroidal winding," *IEEE Transactions on Energy Conversion*, pp. 1752–1763, 2022, doi: 10.1109/TEC.2021.3138465.
- [4] B. Habib, B. Zinelabidine, and B. Abdelkader, "Comparison study between neural STSM and ANFIS-STSM method in DPC control scheme of DFIG-based dual-rotor wind turbines," *International Journal of Energy and Environment*, vol. 14, pp. 33–46, Dec. 2020, doi: 10.46300/91012.2020.14.7.
- [5] R. Resmi, V. Vanitha, T. Nambiar, and S. K. Kottayil, "Design and implementation of brushless doubly fed induction machine with new stator winding configuration," *Wind Engineering*, vol. 45, no. 1, pp. 11–23, Feb. 2021, doi: 10.1177/0309524X19868423.
- [6] Z. Zhang, S. Yu, F. Zhang, S. Jin, and X. Wang, "Electromagnetic and structural design of a novel low-speed high-torque motor with dual-stator and PM-reluctance rotor," *IEEE Transactions on Applied Superconductivity*, vol. 30, no. 4, pp. 1–5, Jun. 2020, doi: 10.1109/TASC.2020.2977286.




- [7] M. Zerzeri and A. Khedher, "Optimal speed–torque control of doubly-fed induction motors: Analytical and graphical analysis," *Computers & Electrical Engineering*, vol. 93, p. 107258, Jul. 2021, doi: 10.1016/j.compeleceng.2021.107258.
- [8] D. Talebi, M. C. Gardner, S. V. Sankarraman, A. Daniar, and H. A. Toliyat, "Electromagnetic design characterization of a dual rotor axial flux motor for electric aircraft," *IEEE Transactions on Industry Applications*, vol. 58, no. 6, 2022, doi: 10.1109/TIA.2022.3191300.
- [9] H. Benbouhenni, I. Colak, N. Bizon, and E. Abdelkarim, "Fractional-order neural control of a DFIG supplied by a two-level PWM inverter for dual-rotor wind turbine system," *Measurement and Control*, vol. 57, no. 3, pp. 301–318, Mar. 2024, doi: 10.1177/00202940231201375.
- [10] A. Al-Mahturi and H. Wahid, "Optimal tuning of linear quadratic regulator controller using a particle swarm optimization for two-rotor aerodynamical system," *International Journal of Electronics and Communication Engineering*, vol. 11, no. 2, pp. 196–202, 2017, [Online]. Available: <https://www.researchgate.net/publication/323532875>
- [11] H. Benbouhenni *et al.*, "Dynamic performance of rotor-side nonlinear control technique for doubly-fed multi-rotor wind energy based on improved super-twisting algorithms under variable wind speed," *Scientific Reports*, vol. 14, no. 1, 2024, doi: 10.1038/s41598-024-55271-7.
- [12] B. Ladghem-Chikouche, K. Boughrara, F. Dubas, L. Roubache, and R. Ibtouen, "Semi-analytical magnetic field calculation for dual-rotor permanent-magnet synchronous machines by using hybrid model," *IEEE Transactions on Magnetics*, vol. 58, no. 1, pp. 1–10, Jan. 2022, doi: 10.1109/TMAG.2021.3127359.
- [13] Z. Zhang, S. Yu, F. Zhang, S. Jin, and X. Wang, "Electromagnetic and structural design of a novel low-speed high-torque motor with dual-stator and PM-reluctance rotor," *IEEE Transactions on Applied Superconductivity*, vol. 30, no. 4, pp. 1–5, Jun. 2020, doi: 10.1109/TASC.2020.2977286.
- [14] H. Benbouhenni, "Synergetic control theory scheme for asynchronous generator based dual-rotor wind power," *Journal of Electrical Engineering, Electronics, Control and Computer Science*, vol. 7, no. 3, pp. 19–28, 2021.
- [15] Y. Wang, Q. Zheng, Z. Xu, and H. Zhang, "A novel control method for turboshaft engine with variable rotor speed based on the Ngdot estimator through LQG/LTR and rotor predicted torque feedforward," *Chinese Journal of Aeronautics*, vol. 33, no. 7, pp. 1867–1876, Jul. 2020, doi: 10.1016/j.cja.2020.01.009.
- [16] J. Zhang, B. Zhang, G. Feng, and B. Gan, "Design and analysis of a low-speed and high-torque dual-stator permanent magnet motor with inner enhanced torque," *IEEE Access*, vol. 8, pp. 182984–182995, 2020, doi: 10.1109/ACCESS.2020.3028425.
- [17] H. Benbouhenni and N. Bizon, "Terminal synergetic control for direct active and reactive powers in asynchronous generator-based dual-rotor wind power systems," *Electronics*, vol. 10, no. 16, p. 1880, Aug. 2021, doi: 10.3390/electronics10161880.
- [18] C. Tong, J. Lang, J. Bai, P. Zheng, and D. Ma, "Deadbeat-direct torque and flux control of a brushless axial-flux magnetic-gear double-rotor machine for power-splitting HEVs," *IEEE Transactions on Industrial Electronics*, vol. 70, no. 9, pp. 8734–8745, Sep. 2023, doi: 10.1109/TIE.2022.3213888.
- [19] D. H. Didane, N. Rosly, M. F. Zulkafli, and S. S. Shamsudin, "Performance evaluation of a novel vertical axis wind turbine with coaxial contra-rotating concept," *Renewable Energy*, vol. 115, pp. 353–361, Jan. 2018, doi: 10.1016/j.renene.2017.08.070.
- [20] J. Taghinezhad, R. Alimardani, M. Masdari, and E. Mahmoodi, "Performance optimization of a dual-rotor ducted wind turbine by using response surface method," *Energy Conversion and Management: X*, vol. 12, p. 100120, Dec. 2021, doi: 10.1016/j.ecmx.2021.100120.
- [21] X. Chen, H. Zhang, C. Zou, J. Zhai, and Q. Han, "Research on the prediction method of unbalance responses of dual-rotor system based on surrogate models," *SN Applied Sciences*, vol. 2, no. 1, p. 12, Jan. 2020, doi: 10.1007/s42452-019-1818-0.
- [22] C. Fu, G. Feng, J. Ma, K. Lu, Y. Yang, and F. Gu, "Predicting the dynamic response of dual-rotor system subject to interval parametric uncertainties based on the non-intrusive metamodel," *Mathematics*, vol. 8, no. 5, p. 736, May 2020, doi: 10.3390/math8050736.
- [23] M. Kreutz *et al.*, "Convolutional neural network with dual inputs for time series ice prediction on rotor blades of wind turbines," *Procedia CIRP*, vol. 104, pp. 446–451, 2021, doi: 10.1016/j.procir.2021.11.075.
- [24] M. Chen and J. P. Hubner, "Prediction of dual-rotor-wing interaction in hover using actuator disk theory," in *AIAA AVIATION 2020 FORUM*, Reston, Virginia: American Institute of Aeronautics and Astronautics, Jun. 2020. doi: 10.2514/6.2020-2793.
- [25] Y. Wang, T. Liu, D. Zhang, and Y. Xie, "Dual-convolutional neural network based aerodynamic prediction and multi-objective optimization of a compact turbine rotor," *Aerospace Science and Technology*, vol. 116, 2021, doi: 10.1016/j.ast.2021.106869.

BIOGRAPHIES OF AUTHORS



Kalpana Anumala    received her first degree from JNTU Hyderabad, Electrical and Electronics Engineering, India, in 2005. She also has a Master's degree from JNTU Hyderabad, Power Electronics, India, in 2012. She is currently a research scholar in the Department of Electrical Engineering at VNRVJIET, JNTU, Hyderabad, India. Her main research interests focus on electric vehicle charging technologies and MATLAB simulation. She can be contacted at email: anumala.kalpana@gmail.com.



Ramesh Babu Veligatla    is an Associate Professor in the Electrical and Electronics Engineering Department at VNR Vignana Jyothi Institute of Engineering and Technology, JNTU, Hyderabad, Hyderabad, India. He received B.Tech., M.Tech., and Ph.D. degrees in Electrical Engineering from JNTU, Hyderabad, India in 1998, 2004, and 2018, respectively. He has 20+ years of teaching experience in Electrical Engineering. His research interests include electrical machines and drive control. He currently working at VNR Vignana Jyothi Institute of Engineering and Technology, JNTU, Hyderabad, India. He can be contacted at email: rameshbabu0506@gmail.com.